Capturing ultrafast magnetic dynamics by time-resolved soft x-ray magnetic circular dichroism

Kou Takubo,[1, a)] Kohei Yamamoto,[1] Yasuyuki Hirata,[1] Yuichi Yokoyama,[1] Yuya Kubota,[1] Shingo Yamamoto,[1] Susumu Yamamoto,[1] Iwao Matsuda,[1] Shik Shin,[1] Takeshi Seki,[2] Koki Takanashi,[2] and Hiroki Wadati[1]

[1)] *Institute for Solid State Physics, University of Tokyo, Kashiwanoha 5-1-5, Chiba 277-8581, Japan*

[2)] *Institute for Materials Research, Tohoku University, Katahira 2-1-1, Sendai 980-8577, Japan*

(Dated: 13 January 2017)

Experiments of time-resolved x-ray magnetic circular dichroism (Tr-XMCD) and resonant x-ray scattering at a beamline BL07LSU in SPring-8 with a time-resolution of under 50 ps are presented. A micro-channel plate is utilized for the Tr-XMCD measurements at nearly normal incidence both in the partial electron and total fluorescence yield (PEY and TFY) modes at the $L_{2,3}$ absorption edges of the $3d$ transition-metals in the soft x-ray region. The ultrafast photo-induced demagnetization within 50 ps is observed on the dynamics of a magnetic material of FePt thin film, having a distinct threshold of the photon density. The spectrum in the PEY mode is less-distorted both at the $L_{2,3}$ edges compared with that in the TFY mode and has the potential to apply the sum rule analysis for XMCD spectra in pump-probed experiments.

arXiv:1701.03156v1 [physics.ins-det] 10 Jan 2017

Control of electron, magnetic, and lattice states by optical excitations in magnetically ordered materials has attracted considerable attention due to their potential applications in electronic and magnetic recording media functioning on an ultrafast time scale below nanosecond (ns, 10^{-9} second, GHz range), since the observation of the ultrafast demagnetization in Ni within 1 picosecond (ps), which was explored by time-resolved magneto-optical Kerr effect (MOKE) studies.[1] The ultrafast photo-induced changes of magnetic states are non-equilibrium phenomena and several mechanisms have been proposed to understand them.[2,3] These mechanism require cooperative effects, inevitably having a threshold of the photon density.

To capture their non-equilibrium dynamics, ultrafast time-resolved experiments have been carried out using ultra-short laser pulses.[3] Recently, the development of a bunched synchrotron light source and x-ray free electron lasers have enabled investigation of the dynamic phenomena with element selectivity by tuning the photon energy of the x-ray to the absorption edges of the constituent elements.[4–12] Especially, time-resolved soft x-ray spectroscopy has many unique characteristics, such as element specificity, chemical specificity and surface sensitivity, which make them versatile for application in a wide range of scientific fields including spintronics and environmental science. Owing to its importance, various time-resolved soft x-ray spectroscopy studies have been carried out.[13–21] The time-resolved x-ray magnetic circular dichroism (Tr-XMCD) and resonant soft x-ray scattering (Tr-RSXS) measurements for magnetic and electronic materials have been conducted in LCLS,[11,12] ALS,[6] and BESSY II slicing facilities.[8,9,13–18] The time-resolved x-ray magneto optical Kerr effect (XMOKE) measurements have also been conducted in FERMI.[10]

XMCD at the $L_{2,3}$ absorption of transition-metals is a powerful tool to evaluate the magnetic moments at the specific sites.[22,23] Sum rules for XMCD in x-ray absorption spectroscopy (XAS) allow us to determine the orbital and spin contributions to the magnetic moments from the integrated XMCD. The static soft XAS and XMCD in the total electron yield (TEY) mode are the most functional and simple methods, in which the photo-current induced by x-ray absorption is measured. In the pump-probe experiments, however, the photo-current induced by the pump laser exceeds that by the probe x ray. Thus, previous pump-probe XAS and XMCD experiments conduced in ALS, LCLS, and BESSY II have been performed in the transmission setting for thin films on transmissive substrates or foils like Si_3N_4, Al and so forth.[5,6,8,14,16,17] However, the good qualities of magnetic materials such as a perpendicular magnetic FePt thin film are unable to be achieved on the transparent Si_3N_4. The x-ray reflectivity and XMOKE measurements have also been performed for non-transparent thin films or bulk samples but with rather grazed settings for their magnetized axis.[9,10,18]

To measure non-transmissive as-grown samples at nearly normal incidence, we presents new settings for Tr-XAS and Tr-XMCD in the partial electron yield (PEY) and total fluorescence yield (TFY) modes. The PEY mode, in which the emitted photoelectrons are measured, is rather surface sensitive but these spectra are known to usually be similar to those obtained in the TEY.[24] On the other hand, the TFY mode, in which the fluorescence of an x-ray is measured, is rather bulk sensitive compared to EY. Despite its bulk-sensitivity, the relationship between FY and the absorption coefficient is non-trivial and saturation effects become important in the TFY.[25–27] The saturation effects in the TFY often change the ratio of XMCD at the L_2 and L_3 edges and preclude applying the sum rule analysis to them.

FePt thin films have drawn intense research interest owing to their potential for high density recording appli-

[a)] Electronic mail: ktakubo@issp.u-tokyo.ac.jp

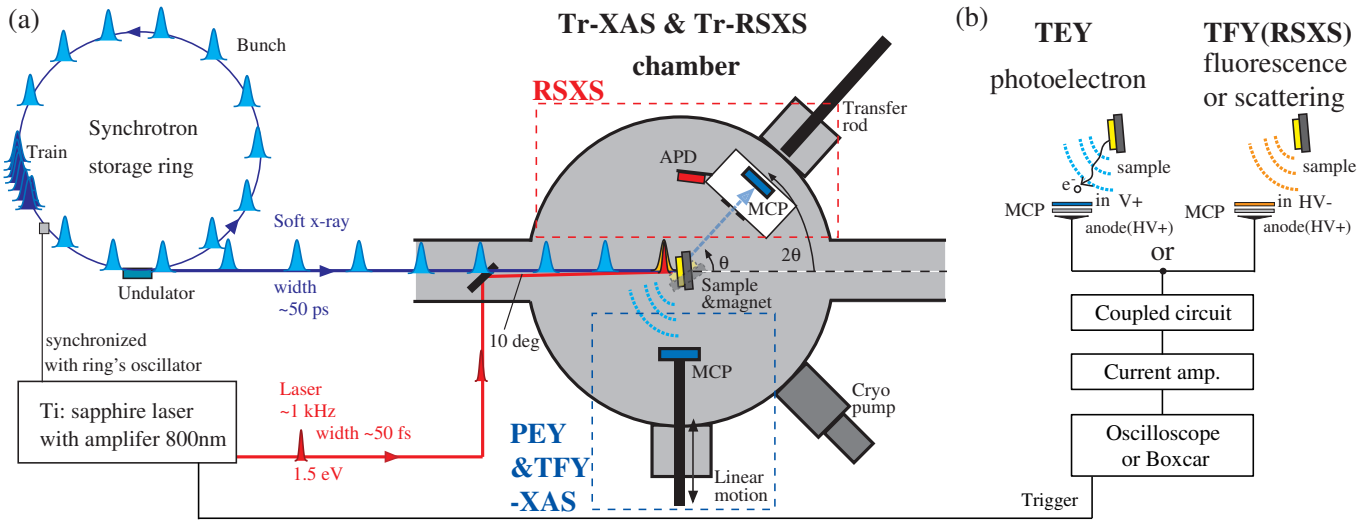

FIG. 1. (a) Overview of the setup for Tr-XAS and Tr-RSXS measurements at BL07LSU of SPring-8. The Ti-sapphire laser with a ∼1 kHz repetition rate, which is synchronized with the bunches of the synchrotron and delayed electronically, is introduced into the experimental chamber. The RSXS measurements are preformed at the $0^\circ < \theta < 90^\circ$ side of the chamber (red dashed box). θ is defined as the angle between the x-ray and sample surface. The XAS and XMCD measurements in the PEY or TFY mode are performed at the $\theta > 90^\circ$ side (blue dashed box). (b) Electrical circuits for the detectors of MCP and APD. The oscilloscope or Boxcar integrator is triggered by the repetition of the laser and used for the data accumulation.

cations by using their magnetism.[28–33] FePt has a high uniaxial magnetic anisotropy when the $L1_0$ ordered structure is formed, and exhibits perpendicular magnetization in $L1_0$-FePt (001) thin films, which makes it a candidate for heat-assisted magnetic recording (HAMR),[34] which is an already-working technology that incorporates laser heating into the recording process. Recently, it has been shown that proper heat-sink layers optimize the recording-time window down to 0.2 ns in HAMR of FePt.[35] The challenge of achieving shorter recording-time has led to an intensive research of the ultrafast magnetization dynamics. Very recently, Lambert *et al.* have showed that circularly polarized laser pulses can induce a small helicity-dependent magnetization in FePtAgC granular film.[36] This finding suggests the possibility of all-optical switching of the magnetism in FePt having very short recording-time windows on the ps time scale. However, the debate on the origin of this effect is ongoing, and more experiments are necessary to clarify if FePt could be switched on the ultrafast time scale.[37,38]

In this letter, the results of Tr-XMCD experiments for as-grown FePt films with non-transmissive substrates are reported. By virtue of the pump-probe technique, a photo-induced ultrafast demagnetization at the Fe sites of the FePt thin film having a clear threshold of the photon density is clarified within the experimental time-resolution of 50 ps for Tr-XMCD at SPring-8.

Figure 1 shows an overview of the experimental setup for Tr-XAS, Tr-XMCD, and Tr-RSXS measurements in the soft x-ray region at BL07LSU of SPring-8.[39] Tr-RSXS is performed at the $\theta < 90^\circ$ side of the experimental chamber. θ is the angle between the x-ray and sample-surface as the standard definition of x-ray diffraction. The scattering is detected by the micro-channel plate (MCP) or avalanche photodiode (APD) installed on the 2θ motion of the diffractometer.[40] On the other hand, XAS and XMCD in the PEY or TFY modes are measured at the $\theta > 90^\circ$ side of the chamber. Emitted photoelectrons or x-ray fluorescence are caught by another MCP topped on the linear motion, which could be positioned as close as ∼2 cm from the sample surface. The femtosecond Ti:sapphire laser with a wavelength of ∼ 800 nm housed at the laser station of BL07LSU[19,20,39] is introduced into the XAS and RSXS chamber. The laser irradiates samples 10° below the x-ray and photo-induced dynamics of the electronic and structural evolutions are examined by means of the pump-probed technique. The laser pulses with ∼ 1 kHz repetition rate are synchronized with selected bunches of the synchrotron and delayed electronically. The spatial and temporal overlap between the x-ray and laser beam are monitored using the photodiode on the manipulator. The pulse width of the Ti:sapphire laser is ∼ 50 fs. On the other hand, the single bunch width of the x-rays in the H-mode and F-mode at SPring-8[42] is ∼ 50 ps, which limits the experimental time-resolution. Figure 2 shows an example of the time-profile of the signals in the F-mode. The signals of the MCP or APD are amplified and gated on the oscilloscope or Boxcar integrator which is triggered by the laser pulses [See Fig.1 (b)].

A chevron-type (dual-plate) MCP[41] is leveraged for XAS and XMCD measurements in the PEY and TFY modes. Each surface channel of the MCP detects both charged particles (photoelectrons) and energetic photons (x-ray) and amplifies them as the electric currents. When a positive voltage is applied to MCP-in terminal of the

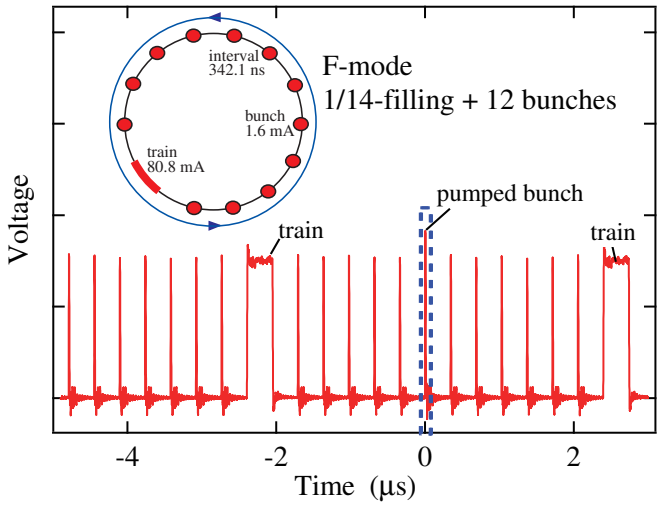

FIG. 2. An example of signal output observed on the oscilloscope during the time-resolved measurements in the F-mode at SPring-8. The example corresponds to the data at t=30 ps taken with the μ^- polarization, shown in Fig.4 (a). The dashed box denotes the gated region. Inset shows the bunch configuration of the F-mode.[42]

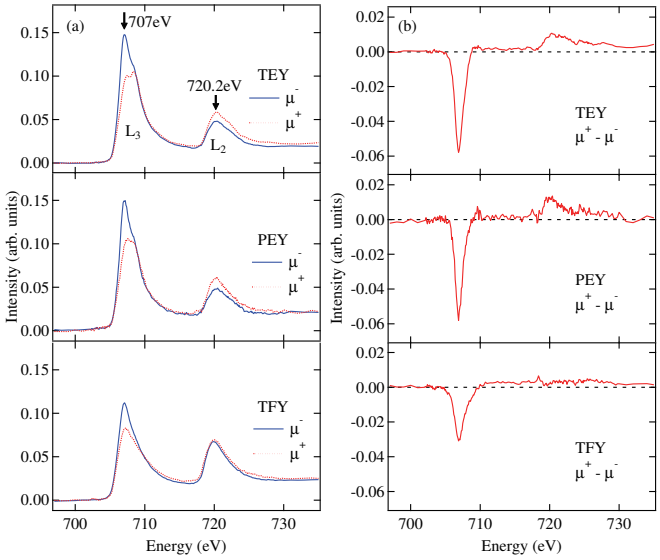

FIG. 3. Static XMCD spectra of the FePt thin film taken in the TEY (top), PEY (middle), and TFY (bottom) modes at room temperature. (a) XAS spectra taken at the μ^+ and μ^- polarization. The spectra are normalized by the area between 700 and 740 eV. The arrows denote the energies used in the time-resolved measurements for the $L_{2,3}$ edges. (b) XMCD intensities.

surface plate, both the photoelectrons and x-ray fluorescence are detected, as illustrated in Fig. 1(b). However, since the current induced by the photoelectron is much larger than that by x-ray, the spectrum can be regarded to arise from the PEY. Alternatively, when a negative high voltage (HV) is applied to the MCP-in, the photoelectrons are bounded and only the fluorescence reaches to MCP. In this case, the TFY spectrum is obtained.

A FePt (001) thin film with the thickness of 50 nm was epitaxially grown at 500°C on an MgO (100) single crystal substrate in an ultrahigh vacuum magnetron sputtering system.[31] The high temperature deposition process promoted the $L1_0$ ordering of FePt, resulting in the perpendicular magnetization. Right and left circularly polarized high-brilliant x-rays (μ^+ and μ^-) for the XMCD measurement were obtained by combinations of vertical figure-8 and horizontal figure-∞ undulators in BL07LSU.[39] The x-ray beams were focused using a mirror and its size was 100 μm × 200 μm on the sample. The magnetic field was applied by a 260mT permanent magnet placed behind the substrate. XMCD was measured at 10 degrees off normal incidence ($\theta = 100°$). The laser was linearly polarized and focused to a size $\phi \sim$ 1mm^2 on the sample.

Figure 3 shows the static XMCD spectra at the Fe $L_{2,3}$ edges for the FePt thin film in the TEY, PEY, and TFY modes. Intense XMCD was observed both at the $L_{2,3}$ edges, ∼-40% at 707 eV and ∼6% at 720.2eV for the original μ^- XAS in TEY and PEY. A spectral difference between the TEY and PEY mode is barely observable. On the other hand, XMCD at the L_2 edge in the TFY mode is scarcely observed owing to the distortion caused by the saturation effect, although TFY has a bulk-sensitivity. Using the sum rules, the magnetic moments at the Fe site are estimated to be m_{spin}=2.63μ_B and $m_{orbital} = 0.10\mu_B$ for TEY, and m_{spin}=2.74μ_B and $m_{orbital} = 0.15\mu_B$ for PEY, respectively. Here, the number of the 3d electrons was assumed to be n_{3d}=6.6. These values are basically consistent with previous studies,[43–48] while it has already been argued that there were some systematic discrepancies arising from the errors in the background subtraction procedures.[48] On the other hand, the magnetic moments are estimated to be m_{spin}=1.53μ_B and $m_{orbital} = 0.08\mu_B$ for the TFY spectra, which exhibited a large discrepancy arising from their strong distortion.

The photo-induced dynamics of the FePt thin film were examined in the less-distorted PEY mode. The time-evolutions of the FePt thin film with 16 mJ/cm^2 laser irradiation are given in Fig. 4 (a) at $h\nu$=707.0 eV (L_3 edge) and (b) at 720.2 eV (L_2 edge), respectively. As can be seen, almost similar time-evolutions are observed for the Fe $L_{2,3}$ edges. XMCD, namely the difference of the intensities at μ^+ and μ^-, decreases immediately after the pumped pulse irradiation both at the Fe $L_{2,3}$ edges. XMCD exhibited a reduction in ts intensity by ∼90% of the original value at both the $L_{2,3}$ edges ∼30 ps after the pump pulse. Then the XMCD exhibits a slow recovery of the magnetization but is not recovered to the original value even at t=1500 ps, which is completed before the next bunch arrives after ∼342 ns. The time-evolutions are fitted by the following function

$$I(t) = I_1 \exp(-t/\tau_{fast}) + I_2[1 - \exp(-t/\tau_{relax})], \quad (1)$$

convoluted with the Gaussian response function of the

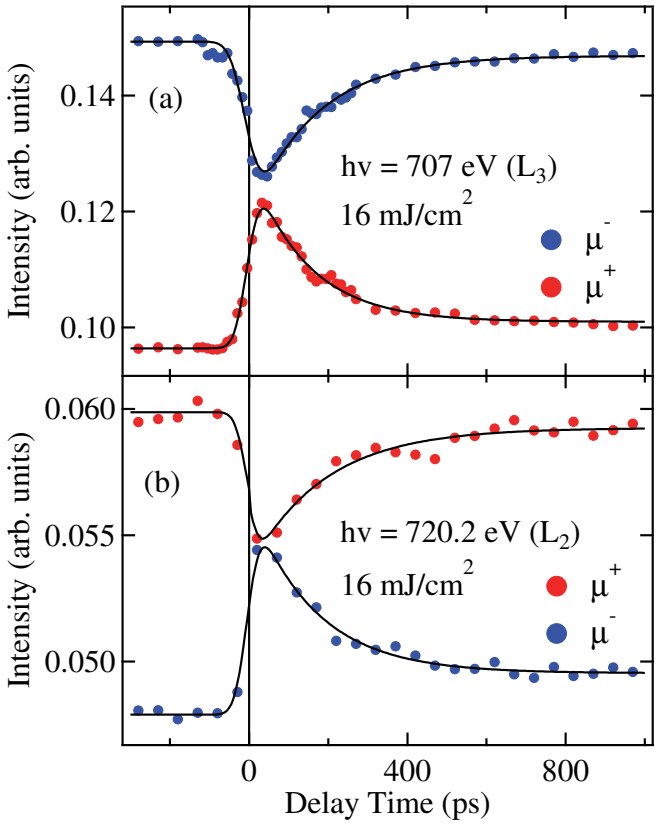

FIG. 4. Time-evolutions of XMCD taken in the PEY mode at (a) L_3 ($h\nu$=707.0 eV) and (b) L_2 ($h\nu$=720.2 eV) edges for the FePt thin film at room temperature. The power density of the laser is 16 mJ/cm^2. The solid lines denote the fitting results (see text).

time-resolution (τ_{Gauss}=50 ps). The 4 time-evolutions can be fitted with similar time constants of $\tau_{fast} = 25 \pm 10$ ps and $\tau_{relax} = 150 \pm 10$ ps (solid lines in Fig. 4). On analysis, the photo-induced demagnetization occurs within the experimental time resolution < 50 ps after the pump pulse, and is relaxed with a time constant of $\sim$150 ps. It should be noted that the time constant of $\sim$ 150 ps for the demagnetization recovery in the FePt thin film is much slower than that observed in the elementary metals Fe, Ni, and so forth of $\sim$10 ps,[3] and similar to the slow recovery of several-hundreds ps time scale observed for the intermetallic GdFeCo[3,14] and Co/Pt multi layers,[49] which also show magnetization reversals induced by the laser pulses.

Figure 5 gives the Tr-XMCD intensities (μ^+ and μ^-) at t=30 ps as a function of the laser fluence. The threshold-like behaviour is observed around 6.5$\pm$0.7mJ/cm^2 denoted by the crossing point of the dashed lines, indicating that this effect is a photo-induced cooperative phenomenon and not a simple thermal effect.[2,5,18]

Here, we report the advantage of Tr-XAS and XMCD in the PEY and TFY modes at nearly normal incidence for non-transmissive thin films or bulk samples. The less-distorted PEY method will provide an opportunity

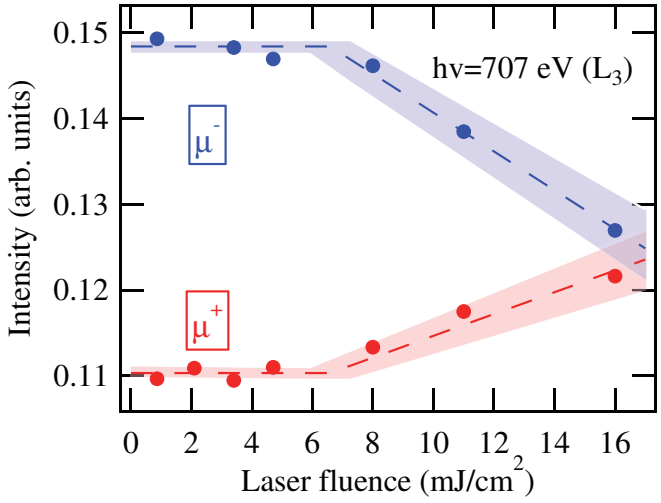

FIG. 5. Laser-fluence dependence of Tr-XMCD intensities (μ^+ and μ^-) at t=30 ps on the L_3 edge ($h\nu$=707.0 eV) for the FePt thin film at room temperature. The dashed lines denote results of the linear fittings having a threshold. Shades indicate the error of the fittings.

for applying a sum rule analysis to XMCD spectra in the ultrafast pump-probed spectroscopy for various magnetic materials, which would be very useful to explore the all-optical switching in spintronics devices such as FePt, Co/Pt multi-layers and so forth. On the other hand, the bulk sensitive TFY method will allow us to measure the dynamics of bulk samples showing various quantum phenomena including high-T_c superconductors, heavy fermion metals and sof forth.

In conclusion, we have studied the photo-induced magnetic dynamics of the FePt thin films at the Fe site using the Tr-XMCD technique at nearly normal incidence. The ultrafast photo-induced demagnetization within 50 ps, which is limited by the width of the bunches from the synchrotron, is clarified with a distinct threshold-like behaviour MCP has been used for Tr-XMCD both in the electron and fluorescence yield modes at the $L_{2,3}$ edges of the 3d transition-metals in the soft-x-ray region. The spectrum in the PEY mode is less distorted and basically similar to that obtained in the TEY mode. No difference of the change ratio is observed between the Fe L_2 and L_3 edges in the time-resolved measurement, taking advantage of the PEY method.

We acknowledge kind supports provided by Dr. T. Ohkochi and Prof. T. Kinoshita. Time-resolved XMCD measurements were performed with the approval of Synchrotron Radiation Research Organization, the University of Tokyo (Proposal No. 2016A7504, 2016A7403, 2016B7403, 2016B7518). This research was supported by the Japan Society the Promotion of Science (JSPS) of Grant-in-Aid for Scientific Research. This work was also partially supported by the Ministry of Education, Culture, Sports, Science and Technology of Japan (X-ray Free Electron Laser Priority Strategy Program).

[1] E. Beaurepaire, J.-C. Merle, A. Daunois, and J.-Y. Bigot, Phys. Rev. Lett. **76**, 4250 (1996).

[2] *Photoinduced Phase Transitions*, edited by K. Nasu, (World Scientific, Singapore, 2004).

[3] A. Kirilyuk, A. V. Kimel, and T. Rasing, Rev. Mod. Phys. **82**, 2731 (2010) and reference there in.

[4] M. Saes, C. Bressler, R. Abela, D. Grolimund, S. L. Johnson, P. A. Heimann, and M. Chergui, Phys. Rev. Lett. **90**, 047403(2003).

[5] A. Cavalleri, M. Rini, H. H. W. Chong, S. Fourmaux, T. E. Glover, P. A. Heimann, J. C. Kieffer, and R. W. Schoenlein, Phys. Rev. Lett. **95**, 067405 (2005).

[6] C. Stamm, T. Kachel, N. Pontius, R. Mitzner, T. Quast, K. Holldack, S. Khan, C. Lupulescu, E. F. Aziz, M. Wietstruk, H. A. Dürr, and W. Eberhardt, Nat. Mater. **6**, 740-743 (2007).

[7] T. Sato, S. Nozawa, K. Ichiyanagi, A. Tomita, M. Chollet, H. Ichikawa, H. Fujii, S. Adachi, and S. Koshihara, J. Synchrotron Rad. **16**, 110-115 (2009).

[8] C. Boeglin, E. Beaurepaire, V. Halté, V. López-Flores, C. Stamm, N. Pontius, H. A. Dürr, and J.-Y. Bigot, Nature **465**, 458-461 (2010).

[9] K. Holldack, J. Bahrdt, A. Balzer, U. Bovensiepen, M. Brzhezinskaya, A. Erko A, A. Eschenlohr, R. Follath, A. Firsov, W. Frentrup, L. Le Guyader, T. Kachel, P. Kuske, R. Mitzner, R. Müller, N. Pontius, T. Quast, I. Radu, J.-S. Schmidt, C. Schüßler-Langeheine, M. Sperling, C. Stamm, C. Trabant, and A. Föhlisch, J. Synchrotron Rad. **21**, 1090 (2014).

[10] Sh. Yamamoto, M. Taguchi, T. Someya, Y. Kubota, S. Ito, H. Wadati, M. Fujisawa, F. Capotondi, E. Pedersoli, M. Manfredda, L. Raimondi, M. Kiskinova, J. Fujii, P. Moras, T. Tsuyama, T. Nakamura, T. Kato, T. Higashide, S. Iwata, S. Yamamoto, S. Shin, and I. Matsuda, Rev. Sci. Instr. **86**, 083901 (2015).

[11] D. J. Higley, K. Hirsch, G. L. Dakovski, E. Jal, E. Yuan, T. Liu, A. A. Lutman, J. P. MacArthur, E. Arenholz, Z. Chen, G. Coslovich, P. Denes, P. W. Granitzka, P. Hart, M. C. Hoffmann, J. Joseph, L. Le Guyader, A. Mitra, S. Moeller, H. Ohldag, M. Seaberg, P. Shafer, J. Stöhr, A. Tsukamoto, H.-D. Nuhn, A. H. Reid, H. A. Dürr, and W. F. Schlotter, Rev. Sci. Instr. **87**, 033110 (2016).

[12] C. Bostedt, S. Boutet, D. M. Fritz, Z. Huang, H. Ja Lee, H. T. Lemke, A. Robert, W. F. Schlotter, J. J. Turner, and G. J. Williams, Rev. Mod. Phys. **88**, 015007 (2016).

[13] K. Holldack, N. Pontius, E. Schierle, T. Kachel, V. Soltwisch, R. Mitzner, T. Quast, G. Springholz, and E. Weschke, Appl. Phys. Lett. **97**, 062502 (2010).

[14] I. Radu, K. Vahaplar, C. Stamm, T. Kachel, N. Pontius, H. A. Dürr, T. A. Ostler, J. Barker, R. F. L. Evans, R. W. Chantrell, A. Tsukamoto, A. Itoh, A. Kirilyuk, Th. Rasing, and A. V. Kimel, Nature **472**, 205-208 (2011).

[15] M. Wietstruk, A. Melnikov, C. Stamm, T. Kachel, N. Pontius, M. Sultan, C. Gahl, M. Weinelt, H. A. Dürr, and U. Bovensiepen, Phys. Rev. Lett. **106**, 127401 (2011).

[16] N. Bergeard, V. López-Flores, V. Halté, M. Hehn, C. Stamm, N. Pontius, E. Beaurepaire, and C. Boeglin, Nat. Commun. **5**, 3466 (2014).

[17] A. Eschenlohr, M. Battiato, P. Maldonado, N. Pontius, T. Kachel, K. Holldack, R. Mitzner, A. Föhlisch, P. M. Oppeneer, and C. Stamm, Nat. Mat. **12**, 332 (2013).

[18] T. Tsuyama, S. Chakraverty, S. Macke, N. Pontius, C. Schüßler-Langeheine, H. Y. Hwang, Y. Tokura, and H. Wadati, Phys. Rev. Lett. **116**, 256402 (2016).

[19] M. Ogawa, S. Yamamoto, Y. Kousa, F. Nakamura, R. Yukawa, A. Fukushima, A. Harasawa, H. Kondoh, Y. Tanaka, A. Kakizaki, and I. Matsuda, Rev. Sci. Instrum. **83**, 023109 (2012).

[20] S. Yamamoto and I. Matsuda, J. Phys. Soc. Jpn, **82**, 021003 (2013).

[21] M. Izquierdo, M. Karolak, C. Trabant, K. Holldack, A. Fhlisch, K. Kummer, D. Prabhakaran, A. T. Boothroyd, M. Spiwek, A. Belozerov, A. Poteryaev, A. Lichtenstein, and S. L. Molodtsov, Phys. Rev. B **90**, 235128 (2014).

[22] C. T. Chen, F. Sette, Y. Ma, and S. Modesti, Phys. Rev. B **42**, 7262 (1990).

[23] B. T. Thole, P. Carra, F. Sette, and G. van der Laan, Phys. Rev. Lett. **68**, 1943 (1992).

[24] J. T. Lau, A. Föhlisch, R. Nietubyć, M. Reif, and W. Wurth, Phys. Rev. Lett. **89**, 057201 (2002).

[25] L. Tröger, D. Arvanitis, K. Baberschke, H. Michaelis, U. Grimm, and E. Zschech, Phys. Rev. B **46**, 3283 (1992).

[26] A. J. Achkar, T. Z. Regier, H. Wadati, Y.-J. Kim, H. Zhang, and D. G. Hawthorn, Phys. Rev. B **83**, 081106(R) (2011).

[27] H. Wadati, A. J. Achkar, D. G. Hawthorn, T. Z. Regier, M. P. Singh, K. D. Truong, P. Fournier, G. Chen, T. Mizokawa, and G. A. Sawatzky, Appl. Phys. Lett. **100**, 193906 (2012).

[28] C. L. Platt, K. W. Wierman, E. B. Svedberg, R. van de Veerdonk, J. K. Howard, A. G. Roy, and D. E. Laughlin, J. Appl. Phys. **92**, 6104 (2002).

[29] T. Shima, K. Takanashi, Y. K. Takahashi, and K. Hono, Appl. Phys. Lett. **81**, 1050 (2002).

[30] C. Moutafis, S. Komineas, C. A. F. Vaz, J. A. C. Bland, T. Shima, T. Seki, and K. Takanashi, Phys. Rev. B **76** 104426 (2007).

[31] T. Seki, H. Iwama, T. Shima, and K. Takanashi, J. Phys. D: Appl. Phys. **44**, 335001 (2011).

[32] S. Bedanta, T. Seki, H. Iwama, T. Shima, and K. Takanashi, Appl. Phys. Lett. **107**, 152410 (2015).

[33] H. Iwama, M. Doi, and T. Shima, Jpn. J. of Appl. Phys. **55**, 7S3 (2016).

[34] D. Weller, A. Moser, L. Folks, M. E. Best, W. Lee, M. F. Tony, M. Schwickert, J. U. Thiele, and M. F. Doerner, IEEE Trans. Magn. **36**, 10 (2000).

[35] D. Weller, O. Mosendz, H. J. Richter, G. Parker, S. Pisana, T. S. Santos, J. Reiner, O. Hellwig, B. Stipe, and B. Terris, *Sub-nanosecond heat assisted magnetic recording of FePt media*, in Ultrafast Magnetism I (Springer, New York, 2015).

[36] C.-H. Lambert, S. Mangin, B. S. D. Ch. S. Varaprasad, Y. K. Takahashi, M. Hehn, M. Cinchetti, G. Malinowski, K. Hono, Y. Fainman, M. Aeschlimann, and E. E. Fullerton, Science **345**, 1337 (2014).

[37] P. Nieves and O. Chubykalo-Fesenko, Phys. Rev. Appl. **5**, 014006 (2016).

[38] M. Berritta, R. Mondal, K. Carva, and P. M. Oppeneer, Phys. Rev. Lett. **117**, 137203 (2016).

[39] S. Yamamoto, Y. Senba, T. Tanaka, H. Ohashi, T. Hirono, H. Kimura, M. Fujisawa, J. Miyawaki, A. Harasawa, T. Seike, S. Takahashi, N. Nariyama, T. Matsushita, M. Takeuchi, T. Ohata, Y. Furukawa, K. Takeshita, S. Goto, Y. Harada, S. Shin, H. Kitamura, A. Kakizaki, M. Oshima, and I. Matsuda, J. Synchrotron Rad. **21**, 352-365 (2014).

[40] Results of the Tr-RSXS measurements will be reported elsewhere.

[41] J. L. Wiza, Nucl. Instr. Methods **162**, 587-601 (1979).

[42] See http://www.spring8.or.jp/en/user/operation_status/schedule/bunch_mode for more information about bunch configuration of SPring-8; accessed 15th Nov. 2016.

[43] C. J. Sun, G. M. Chow, G. H. Fecher, J. S. Chen, H.-J. Lin, and Y. Hwu, Jpn. J. Appl. Phys. **45**, 2539 (2006).

[44] S. Imada, A. Yamasaki, S. Suga, T. Shima, and K. Takanashi, App. Phys. Lett. **90**, 132507 (2007).

[45] M. M. Soares, H. C. N. Tolentino, M. De Santis, A. Y. Ramos, and J. C. Cezar, J. Appl. Phys. **109**, 07D725 (2011).

[46] C. Antoniak, M. E. Gruner, M. Spasova, A. V. Trunova, F. M. Römer, A. Warland, B. Krumme, K. Fauth, S. Sun, P. Entel, M. Farle, and H. Wende, Nat. Commun. **2**, 528 (2011).

[47] D. B. Xu, C. J. Sun, J. S. Chen, S.-W. Han, S. M. Heald, R. A. Rosenberg, and G. M. Chow, J. Appl. Phys. **111**, 07C120 (2012).

[48] M. M. Soares, A. D. Lamirand, A. Y. Ramos, M. De Santis, and H. C. N. Tolentino, Phys. Rev. B **90**, 214403 (2014).

[49] N. Kazantseva, U. Nowak, R. W. Chantrell, J. Hohlfeld, and A. Rebei, Europhys. Lett. **81**, 27004 (2008).